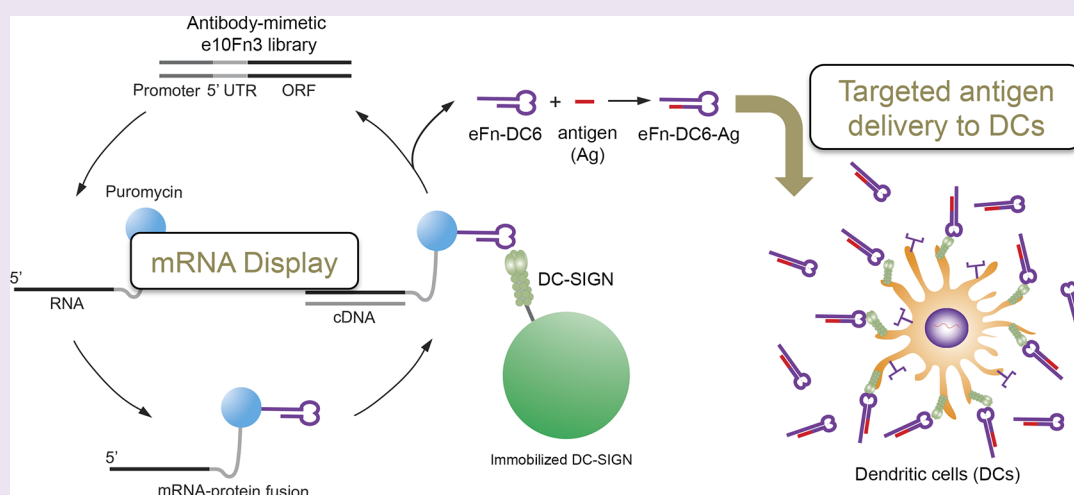


Antibody-Mimetic Ligand Selected by mRNA Display Targets DC-SIGN for Dendritic Cell-Directed Antigen Delivery

Liang Xiao,^{†,‡} Kuo-Chan Hung,^{‡,‡} Terry T. Takahashi,[¶] Kye-Il Joo,[†] Matthew Lim,[†] Richard W. Roberts,^{*,†,¶,||} and Pin Wang^{*,†,‡,§}

[†]Mork Family Department of Chemical Engineering and Materials Science, [‡]Department of Biomedical Engineering, [§]Department of Pharmacology and Pharmaceutical Sciences, [‡]Department of Biochemistry and Molecular Biology, [¶]Department of Chemistry, and ^{||}Department of Biology, University of Southern California, Los Angeles, California 90089, United States



ABSTRACT: Dendritic cell (DC)-based vaccines have shown promise as an immunotherapeutic modality for cancer and infectious diseases in many preclinical studies and clinical trials. Provenge (sipuleucel-T), a DC-based vaccine based on *ex vivo*-generated autologous DCs loaded with antigens, has recently received FDA approval for prostate cancer treatment, further validating the potential of DC-based vaccine modalities. However, direct antigen delivery to DCs *in vivo* via DC-specific surface receptors would enable a more direct and less laborious approach to immunization. In this study, the recombinant extracellular domains (ECD) of human and mouse DC-SIGN (hDC-SIGN and mDC-SIGN) were generated as DC-specific targets for mRNA display. Accordingly, an antibody-mimetic library was constructed by randomizing two exposed binding loops of an expression-enhanced 10th human fibronectin type III domain (e10Fn3). After three rounds of selection against mDC-SIGN, followed by four rounds of selection against hDC-SIGN, we were able to evolve several dual-specific ligands, which could bind to both soluble ECD of human and mouse DC-SIGNs. Using a cell-binding assay, one ligand, eFn-DC6, was found to have high affinity to hDC-SIGN and moderate affinity to mDC-SIGN. When fused with an antigenic peptide, eFn-DC6 could direct the antigen delivery and presentation by human peripheral blood mononuclear cell (PBMC)-derived DCs and stimulate antigen-specific CD8⁺ T cells to secrete inflammatory cytokines. Taken together, these results demonstrate the utility of mRNA display to select protein carriers for DC-based vaccination and offer *in vitro* evidence that the antibody-mimetic ligand eFn-DC6 represents a promising candidate for the development of an *in vivo* DC-based vaccine in humans.

Dendritic cells (DCs) are specialized antigen presenting cells (APCs) that can uptake and process antigens for presentation through the major histocompatibility complex (MHC) and activate naïve T cells.¹ Because of this unique biological role, DCs have been widely exploited to develop DC-based vaccines for protective immunity against bacterial, viral, and fungal infections.² The development of DC-based vaccines has also been one of the major focuses of cancer immunotherapy.^{3,4} Patient-derived DCs are loaded with tumor antigens and subsequently administered back to the patient. This type of autologous cell therapy led to the first FDA-approved cancer vaccine, sipuleucel-T.^{5,6} However, the

tedious procedure for generating the vaccine, its high cost (\$93,000 USD) per patient, and only modest improvement in survival (an average of 4.1 months) could limit its extensive application.^{7,8} A better strategy would be direct and specific loading of antigens onto DCs *in vivo*, which could be achieved by targeting DC-specific cell-surface receptors that facilitate internalization of the bound antigens for antigen presentation.⁹

Received: December 10, 2012

Accepted: February 21, 2013

Published: February 21, 2013

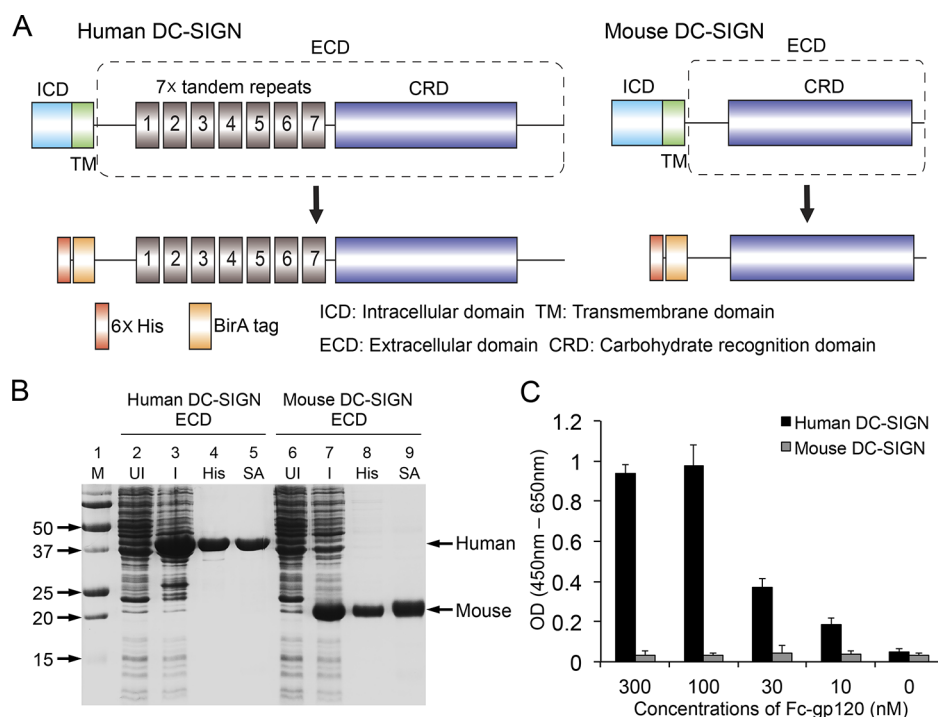


Figure 1. Expression and functional test of human and mouse DC-SIGN extracellular domain (ECD). (A) Schematic representation of the whole length of human and mouse DC-SIGN protein and the ECD of each protein and necessary components that were constructed into the expression vector. (B) SDS-PAGE analysis of recombinant DC-SIGN proteins: Lane 1, M, protein marker (in kDa); Lane 2, UI, uninduced control from bacteria extract; Lane 3, I, IPTG-induced hDC-SIGN ECD; Lane 4, His, His-tag-purified and refolded hDC-SIGN ECD; Lane 5, SA, hDC-SIGN ECD pulled down by streptavidin acrylamide beads; Lane 6, UI, uninduced control from bacteria extract; Lane 7, I, IPTG-induced mDC-SIGN ECD; Lane 8, His, His-tag-purified and refolded mDC-SIGN ECD; Lane 9, SA, mDC-SIGN ECD pulled down by streptavidin acrylamide beads. (C) ELISA analysis of binding of Fc-gp120 protein to refolded DC-SIGN proteins produced by bacterial expression.

C-type lectin receptors (CLRs) constitute a well-studied family of proteins that have specific expression pattern on APCs and can uniquely capture and endocytose antigens.¹⁰ Although several CLRs have been reported as targets for antigen loading, DC-specific ICAM3-grabbing non-integrin (DC-SIGN or CD209) is a promising target for DC-specific antigen delivery because it is predominantly expressed on DCs, allowing for higher targeting efficiencies and fewer side effects.¹¹ Furthermore, studies have shown that anti-DC-SIGN antibody-based antigen loading can elicit both naïve and memory T cell responses *in vitro*.¹² Multiple mouse homologues of human DC-SIGN (hDC-SIGN) have been identified by their sequence similarities and genetic loci; one of these homologues, having the highest homology to hDC-SIGN, was named mouse DC-SIGN (mDC-SIGN or CD209A/CIRE). mDC-SIGN localizes syntenically to hDC-SIGN and is expressed on a subset of DCs in a manner similar to hDC-SIGN.¹³ The ability of mDC-SIGN to internalize a bound ligand has been the subject of conflicting reports;^{14,15} however, lentiviral vectors targeting mDC-SIGN have been successfully demonstrated to specifically deliver antigen to mouse DCs and establish antigen-specific immune responses *in vivo*.^{16–19} Thus, in an effort to establish preclinical animal models and subsequent translation to clinical human studies for DC-SIGN-targeted vaccine development, it would be advantageous to identify highly specific ligands that can recognize both hDC-SIGN and mDC-SIGN.

In this study, we utilized mRNA display of an antibody-mimetic e10Fn3 library to identify DC-SIGN-specific ligands. This antibody-mimetic e10Fn3 molecule has several advantages over humanized antibodies. First of all, it has a relatively small size (~10 kDa) to be used as scaffold for mRNA display and

smaller size is better for tissue penetration that is a preferable property for vaccine delivery. Second, it can be easily produced by bacteria cells in large amounts, greatly reduce the cost for future medical application. mRNA display is a powerful *in vitro* selection technique that can evolve antibody-mimetic ligands with high specificity and affinity to targets of interest.^{20–24} Theoretically, antibody-mimetic libraries based on a scaffold derived from fibronectin (e.g., the 10Fn3 library) of $>10^{12}$ molecules can be generated using mRNA display.^{25–27} In order to improve the expression and stability of the 10Fn3 library, a new e10Fn3 library was designed based on the wild-type 10Fn3.²⁸ The e10Fn3 scaffold is derived from the human fibronectin protein, thereby reducing the concern of undesirable immune responses against targeting ligands when used to direct *in vivo* vaccine delivery in humans.

Herein we report our efforts to design functional ligands with dual specificity against the extracellular domains of hDC-SIGN and mDC-SIGN. Three rounds of mDC-SIGN-based selection followed by four rounds of hDC-SIGN-based selection resulted in one molecule, eFn-DC6, which recognizes both hDC-SIGN and mDC-SIGN. eFn-DC6 was further shown to bind selectively to human DCs and mediate antigen presentation to stimulate antigen-specific T cells *in vitro*.

RESULTS

Identification of DC-SIGN-Specific Ligands via mRNA Display. The extracellular domain of human and mouse DC-SIGN proteins were produced in *E. coli*, purified under denaturing condition and further refolded (Figure 1A and B). It has been reported that hDC-SIGN, rather than mDC-SIGN,

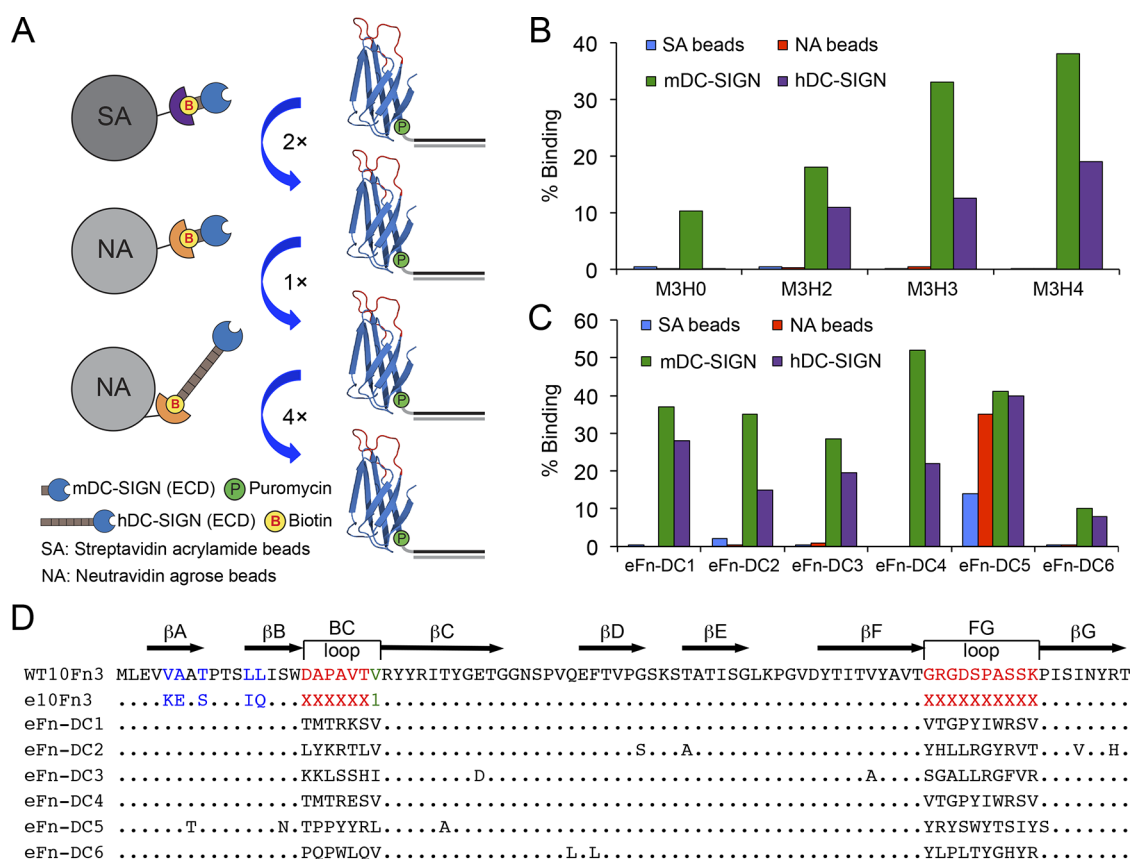


Figure 2. mRNA display selection to identify e10Fn3 variants that can bind to both human and mouse DC-SIGNs. (A) Schematic representation of the procedure for 3 rounds of mDC-SIGN-targeted selection followed by 4 more rounds of hDC-SIGN-targeted selection from the starting of e10Fn3 library. (B) After the 3 rounds of mDC-SIGN-targeted selection, an *in vitro* radiolabeled binding assay was used to assess the binding of each pool from the individual rounds (M3H0, 0 round; M3H2, second round, M3H3, third round; M3H4, fourth round) of hDC-SIGN-based selection toward hDC-SIGN, mDC-SIGN and background beads. (C) An *in vitro* radiolabeled binding assay was used to estimate clones isolated from the last pool (M3H4) for binding to hDC-SIGN, mDC-SIGN, and background beads. (D) Protein sequence comparison among the wild-type 10Fn3, wild-type expression-enhanced 10Fn3 (e10Fn3), and the clones isolated from the last pool (M3H4).

recognizes HIV-1 glycoprotein gp120 by the carbohydrate recognition domain (CRD) located in the extracellular domain (Figure 1B). In order to test whether these refolded proteins could maintain their binding function, a gp120 binding ELISA assay was carried out (Figure 1C). With increasing Fc-gp120 concentration, absorbance for hDC-SIGN ECD also increased and became saturated when the Fc-gp120 concentration reached 100 nM, indicating that refolded hDC-SIGN ECD was able to bind gp120. On the other hand, no obvious binding of mDC-SIGN ECD to Fc-gp120 could be observed, further validating the inability of mDC-SIGN to confer HIV-1 gp120 binding.

In order to generate DC-SIGN-specific ligands with the ability to bind both mouse and human DC-SIGN, we first performed 3 rounds of selection against mDC-SIGN followed by another 4 rounds against hDC-SIGN (Figure 2A). We then tested the different pools' binding against immobilized DC-SIGN. Starting with the M3H0 pool (pool after 3 rounds of selection against mDC-SIGN and 0 round against hDC-SIGN), we observed some affinity to mDC-SIGN (10% binding) but almost no affinity to hDC-SIGN. However, for the M3H4 pool, increasing affinity to both mDC-SIGN (~40%) and hDC-SIGN (~20%) was observed (Figure 2B). These data indicated that the final M3H4 pool contained e10Fn3 scaffolds that could bind to both mDC-SIGN and hDC-SIGN. Thus, the M3H4 pool was sequenced and yielded two dominant clones that were

observed multiple times, as well as five clones that appeared only once. The two dominant clones, eFn-DC1 and eFn-DC7, contain similar BC and FG binding loops; however, eFn-DC7 contains an E21K mutation in the BC loop. Additionally, these two clones displayed similar results for an *in vitro* radiolabeled binding assay (data not shown). Therefore, eFn-DC1 and five singletons (eFn-DC2, eFn-DC3, eFn-DC4, eFn-DC5, and eFn-DC6) were tested further for binding using an *in vitro* radiolabeled binding assay, and their sequences are illustrated in Figure 2D. The binding result shows that five out of six clones (eFn-DC1, eFn-DC2, eFn-DC3, eFn-DC4, and eFn-DC6) bound to both mDC-SIGN and hDC-SIGN; these clones possess higher affinity to mDC-SIGN than hDC-SIGN with very little background binding to beads without target (<1.4%), except for eFn-DC5, which has some background binding (Figure 2C) and was not studied further.

Functional Binding of e10Fn3 DC-SIGN Ligands to Cells Expressing DC-SIGN. From the *in vitro* radiolabeled binding assay, five dual-specific e10Fn3 variants were identified that could bind to bacterially expressed human and mouse DC-SIGN ECD. A C-terminal HA tag was then added to each of these e10Fn3 scaffolds in order to test their binding to either mDC-SIGN (293T.mDCSIGN) or hDC-SIGN (293T.hDCSIGN) overexpressed on 293T cells. After binding, we immunostained and analyzed the cells by flow cytometry. Our data demonstrate that only eFn-DC6 could bind to

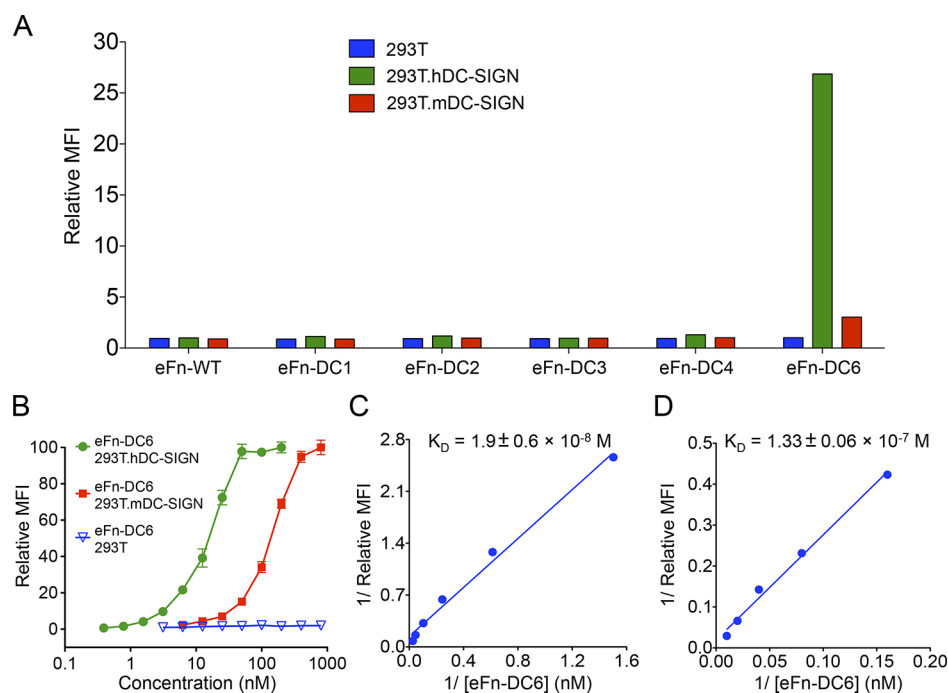


Figure 3. Selection and characterization of isolated e10Fn3 variants for their binding to 293T.hDC-SIGN and 293T.mDC-SIGN cells. (A) 293T, 293T.hDC-SIGN, or 293T.mDC-SIGN cells were incubated at 4 °C with HA-tagged wild-type e10Fn3 (eFn-WT) or selected clones from the last selection pool for 30 min. After the washing step, cell surfaces were stained by anti-HA antibody followed by fluorescence-conjugated secondary antibody for flow cytometry analysis. Relative mean fluorescence intensities (MFIs) were calculated by dividing MFIs by MFI of eFn-WT binding to 293T cells. (B) Various concentrations of eFn-DC6 were incubated with 293T, 293T.hDC-SIGN, or 293T.mDC-SIGN, and relative MFIs were measured. (C, D) Determination of K_D value of eFn-DC6 for its binding to 293T.hDC-SIGN (C) and 293T.mDC-SIGN (D) by Lineweaver–Burk analysis. K_D values were determined by the following equation: $1/(F - F_{\text{back}}) \approx 1/F_{\text{max}} + (K_D/F_{\text{max}})(1/[e\text{Fn-DC6}])$, where F = fluorescence units, F_{back} = background fluorescence, and F_{max} was calculated from the plot.

293T.hDCSIGN cells (relative MFI ≈ 27) and 293T.mDCSIGN cells (relative MFI ≈ 3). The other four clones had no binding to 293T.mDCSIGN or 293T.hDCSIGN cells (relative MFI ≈ 1) (Figure 3A). This result was somewhat surprising since all five e10Fn3 variants bound well in the radiolabeled binding assay and may indicate that these e10Fn3 variants bind to an epitope that is blocked when DC-SIGN is displayed on a cell surface. Nonetheless, since eFn-DC6 could recognize both human and mouse DC-SIGNs, its binding ability was further assessed by varying the concentration of eFn-DC6 (Figure 3B). The binding of eFn-DC6 was specific to human or mouse DC-SIGN, as shown by the absence of significant binding to 293T cells observed even up to 800 nM of eFn-DC6 (Figure 3B). The K_D of the interaction between eFn-DC6 and hDC-SIGN was then determined by Lineweaver–Burk kinetic analysis (Figure 3C), and the K_D was calculated as 19 ± 6 nM. Similarly, the K_D of the interaction between eFn-DC6 and mDC-SIGN was calculated as 133 ± 6 nM (Figure 3D). Therefore, eFn-DC6 was identified as a specific ligand bearing a high affinity to hDC-SIGN and moderate affinity to mDC-SIGN expressed on the surface of mammalian cells.

eFn-DC6-Induced Internalization into DC-SIGN-Expressing Cells. Based on its high and specific affinity to hDC-SIGN, our next experiments focused on interactions between eFn-DC6 and human DC-SIGN. A good antigen carrier should be able to mediate specific binding to a cell-surface receptor with subsequent efficient internalization into cells for antigen processing. Therefore, eFn-DC6 internalization efficiency was quantified by a previously reported assay.²⁹ The

MFIs at 4 and 37 °C were then compared and used to calculate about a 50.2% internalization efficiency (Figure 4A).

It has been shown that DC-SIGN-mediated soluble antigen uptake and HIV virion internalization are clathrin-dependent;^{30,31} however, other studies have indicated that certain antibodies targeting DC-SIGN can enter cells through a clathrin-independent mode.³² In order to facilitate rational design of a targeted antigen delivery strategy, it is necessary to determine the factors mediating the internalization of eFn-DC6 through DC-SIGN. As shown in Figure 4B, significant signal colocalization was observed between eFn-DC6 and clathrin, while colocalization between eFn-DC6 and caveolin-1 was less evident. A significant overlap between eFn-DC6 and clathrin was confirmed using Mander's overlap coefficients and imaging software (Figure 4C).

An efficient vaccine requires delivery of extracellular antigen to APCs and presentation through the MHC molecules, but an antigen must first be internalized to an early endosome. Thus, the early internalization pathway, following the binding of eFn-DC6 to hDC-SIGN, was measured. Accordingly, eFn-DC6 was bound to 293T.hDC-SIGN cells and incubated at 37 °C for 1 h. The cells were then fixed and stained for eFn-DC6, while the marker EEA-1 was used to detect the early endosomes. From the colocalization data, it was clear that eFn-DC6 was internalized to the early endosomes following endocytosis (Figure 4D).

Binding and Internalization of eFn-DC6 into DCs. We demonstrated that eFn-DC6 could specifically bind to hDC-SIGN, mDC-SIGN and mediate internalization into cell lines that overexpress hDC-SIGN. However, it was unknown whether eFn-DC6 could directly target primary DCs and

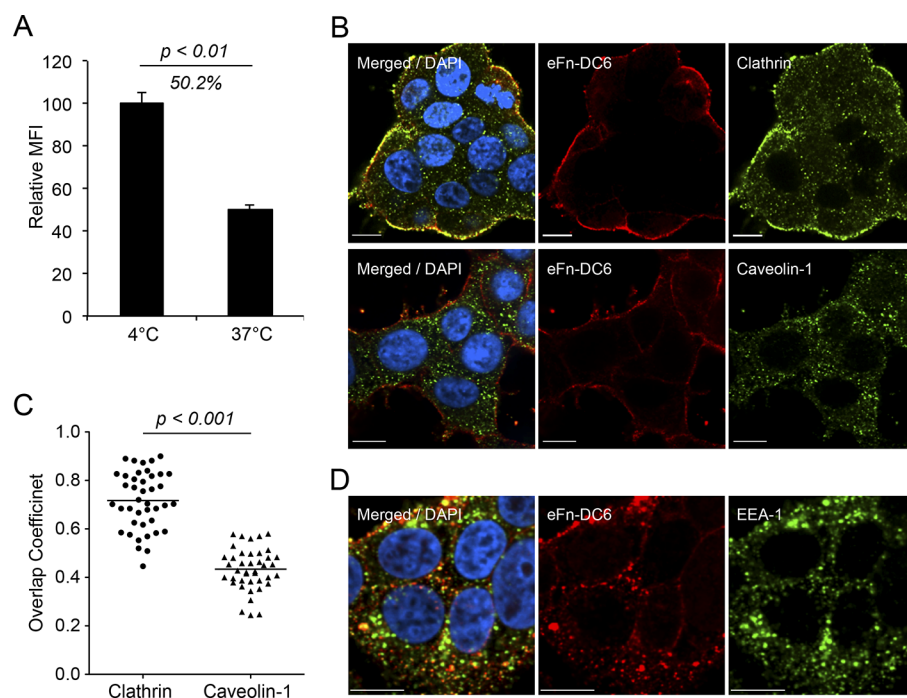


Figure 4. Internalization efficiency and intracellular trafficking of eFn-DC6 in 293T.hDC-SIGN cells. (A) Internalization of eFn-DC6 into 293T.hDC-SIGN cells upon binding to hDC-SIGN. Two groups of 293T.hDC-SIGN cells were incubated at 4 °C with 100 nM eFn-DC6 for 30 min. After washing with PBS, one of them was then incubated at 4 °C, while the other was incubated at 37 °C for 2 h. eFn-DC6 remaining on the cell surface was then stained by anti-HA antibody and analyzed by flow cytometry. Internalization efficiency was calculated from mean fluorescence intensity by the formula $(MFI^{4\text{ }^\circ\text{C}} - MFI^{37\text{ }^\circ\text{C}})/MFI^{4\text{ }^\circ\text{C}}$. (B) Endocytic routes for the cell entry of eFn-DC6. 293T.hDC-SIGN cells were incubated with 100 nM eFn-DC6 for 30 min at 4 °C to synchronize internalization. The cells were then shifted to 37 °C for 15 min, fixed, permeabilized, immunostained with an antibody against HA-tag (red), clathrin (green, upper) or caveolin-1 (green, lower), and counterstained with DAPI (blue). Scale bar represents 10 μm . (C) Quantification of eFn-DC6 colocalized with clathrin or caveolin-1 signals after 15 min of incubation. Mander's overlap coefficients were calculated using Nikon NIS-Elements software by viewing more than 50 cells of each sample. Statistical analysis of p -value was calculated by the one-way ANOVA followed by Bonferroni's multiple comparison test. (D) Intracellular trafficking of eFn-DC6 through early endosomes. 293T.hDC-SIGN cells were incubated with eFn-DC6 for 30 min at 4 °C to synchronize internalization. The cells were then shifted to 37 °C for 30 min, fixed, permeabilized, immunostained with anti-HA tag (red) and anti-EEA1 antibodies (green), and counterstained with DAPI (blue). Scale bar represents 10 μm .

mediate antigen internalization. To evaluate this, we generated DCs from human peripheral blood mononuclear cells (PBMCs). After *in vitro* differentiation, human DCs were incubated with eFn-DC6, co-stained by anti-DC-SIGN and anti-eFn-DC6 antibodies, and analyzed by flow cytometry. More than 90% of human DCs that were derived from PBMCs had a high level of DC-SIGN expression. These DC-SIGN-positive DCs were also recognized by eFn-DC6, but not the original wild-type e10Fn3 (designated as eFn-WT) (Figure 5A). The same assay was conducted using mouse DCs derived from bone marrow. As shown in Figure 5B, around 84% of cells express CD11c and around 17% cells that were detected by eFn-DC6, while eFn-WT could not show any signal. We further conducted a similar internalization assay with human DCs and found that eFn-DC6 utilized a more clathrin-dependent and less caveolin-1-dependent entry pathway into DCs (Figure 5C). Colocalization of eFn-DC6 and early endosome marker EEA-1 was also detected (Figure 5D), suggesting that eFn-DC6-induced internalization could favor antigen presentation to DCs.

Capacity of eFn-DC6 To Mediate Antigen Delivery to DCs *in Vitro*. Next, we evaluated the capacity of eFn-DC6 to mediate antigen delivery to DCs *in vitro*. A new construct was designed whereby a human MHC I restricted antigen epitope from influenza A matrix protein (58GILGFVFTL66)³³ was fused to the C terminus of eFn-DC6 (designated as eFn-DC6-

Ag). The peptide was flanked by 2 arginines to the N terminus and 3 arginines to the C terminus (Figure 6A) based on a previous study indicating that such design could maximize proper antigen processing by proteasomes after internalization.³⁴ A similar design using eFn-WT (designated as eFn-WT-Ag) was also constructed as a control. Previous studies have shown that cells from HLA-A2⁺ adult peripheral blood contain around 1.6% of GILGFVFTL-responsive CD8 T cells from previous exposure to influenza virus. Thus, if eFn-DC6 could be demonstrated to facilitate internalization, processing, and presentation of the influenza antigen peptide by DCs to autologous PBMCs from HLA-A2⁺ adult peripheral blood, then a higher response should be observed over the control. To make this determination, DCs derived from HLA-A2⁺ PBMCs were incubated with eFn-DC6-Ag and as controls, eFn-WT-Ag, eFn-DC6 lacking any antigen (eFn-DC6) or GILGFVFTL peptide antigen. One day later, these three groups of DCs were incubated with autologous PBMCs for 60 h. An ELISPOT assay for human IFN- γ was employed to measure the stimulated T cell responses. As shown in Figure 6B, DCs treated with eFn-DC6 were unable to induce observable responses, while eFn-WT-Ag-treated DCs did generate some response, presumably caused by the random internalization of the antigen. However, eFn-DC6-Ag produced a much higher response (around 150 SFC) than that of eFn-WT-Ag (around 50 SFC). Taken together, our data show that eFn-DC6 not

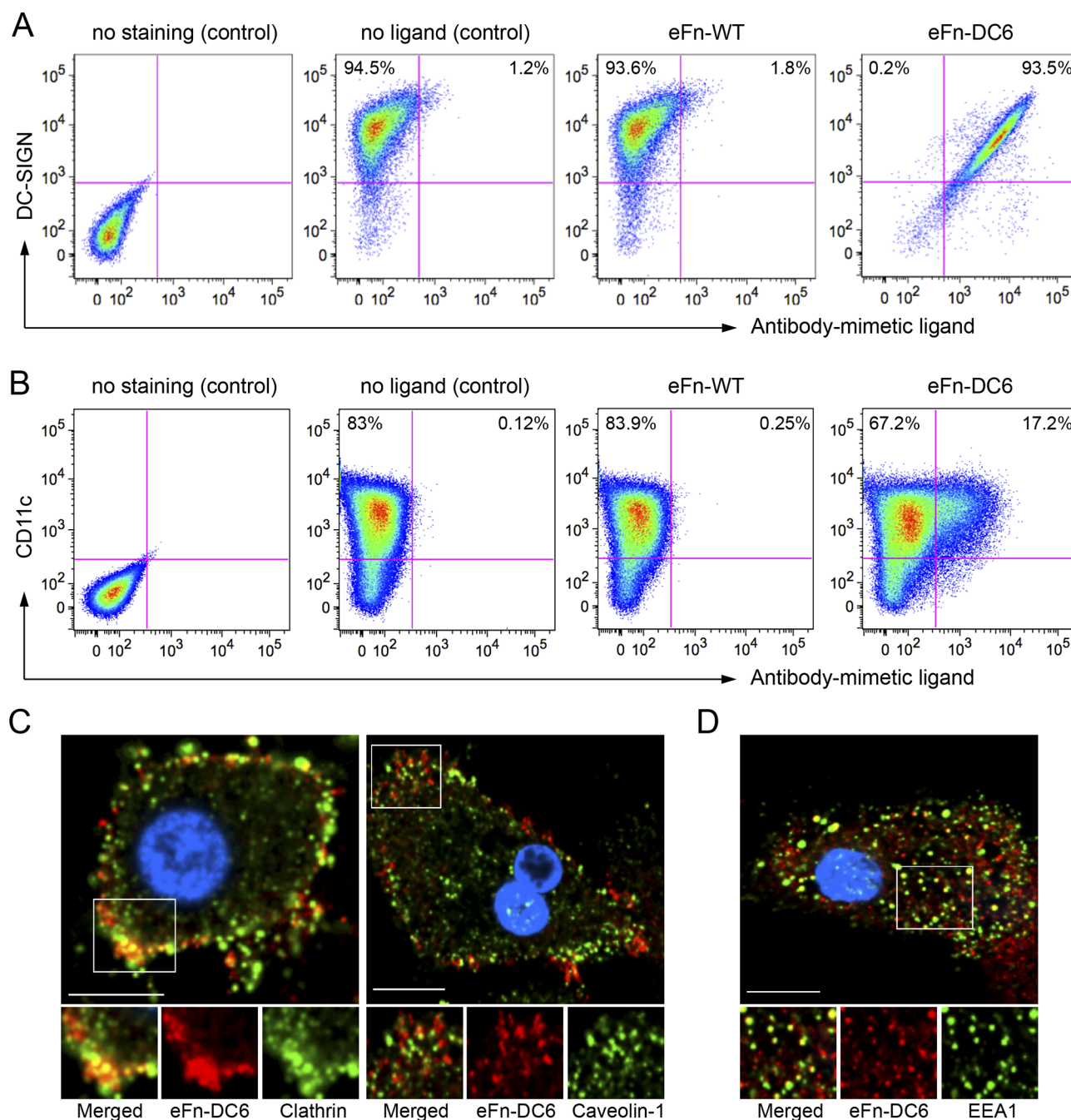


Figure 5. Specific binding and internalization of eFn-DC6 into DCs. (A) Human PBMC-derived DCs were incubated with eFn-DC6 or eFn-WT, stained by anti-HA and anti-DC-SIGN antibodies, and further analyzed by flow cytometry. (B) Mouse bone marrow derived-DCs were incubated with eFn-DC6 or eFn-WT, stained by anti-HA and anti-CD11c antibody, and analyzed. (C, D) Endocytic routes for eFn-DC6 to enter DCs. Human PBMC derived DCs were incubated with eFn-DC6 for 30 min at 4 °C to synchronize internalization. The cells were then shifted to 37 °C for 15 min, fixed, permeabilized, and immunostained with an antibody against HA-tag (red) and clathrin or caveolin-1 (green) (C) or EEA1 (D) and further counterstained with DAPI (blue). Scale bar represents 10 μ m.

only specifically delivered antigens to DCs expressing hDC-SIGN but also induced an antigen-specific immune response.

DISCUSSION

In the present study, we exploited mRNA display and a scaffold library of antibody mimics based on an enhanced tenth fibronectin type III domain (e10Fn3) to design ligands able to specifically bind to the type II C-type lectin DC-SIGN and mediate antigen delivery to DCs. Since human and mouse DC-SIGNs have a homologous carbohydrate recognition domain

(CRD),¹³ we postulated that this design strategy would allow us to identify novel binders with an affinity to both mDC-SIGN and hDC-SIGN. After seven rounds of selection, we found that one ligand, eFn-DC6, displayed dual affinity for hDC-SIGN and mDC-SIGN expressed by mammalian cells when tested in a cell-based binding assay. eFn-DC6 demonstrated excellent affinity to 293T.hDCSIGN cells and moderate affinity to 293T.mDCSIGN cells (Figure 3).

The different binding behaviors for the selected e10Fn3 variants toward DC-SIGNs suggest possible differences in the

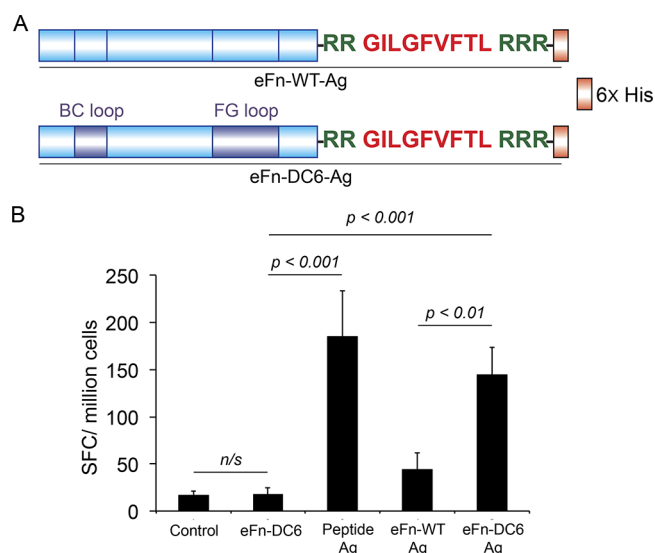


Figure 6. Antigen-specific IFN- γ release of autologous human PBMCs after co-culture with DCs treated by eFn-DC6-fused antigens. (A) Schematic representation of the construction of eFn-DC6 (eFn-DC6-Ag) and eFn-WT (eFn-WT-Ag) fused with an influenza matrix protein antigen peptide GILGFVFTL, which was flanked by 2 arginines to the N terminus and 3 arginines to the C terminus. (B) An ELISPOT assay was used to measure the IFN- γ production by the DC-stimulated CD8⁺ T cells. DCs were first treated with 1 μ M eFn-DC6-Ag, eFn-WT-Ag, eFn-DC6, the GILGFVFTL peptide antigen as a positive control, or not treated as a negative control for 24 h. These treated DCs in each group were further co-cultured with autologous human PBMCs for 60 h. Spot-forming cells (SFC) were measured by an ELISPOT reader. The experiment was performed in triplicate. (n/s: not statistically significant; *p*-value was calculated by one-way ANOVA followed by Bonferroni's multiple comparison test. Error bars represent SD.

structural configuration between the recombinant soluble DC-SIGNS and their cell-surface-displayed counterparts. The recombinant DC-SIGNS were expressed in *E. coli* and refolded in order to obtain functional proteins. The refolded hDC-SIGN was able to recognize the HIV-1 gp120 protein, indicating that hDC-SIGN was folded appropriately and formed a tetramer. It should be noted that multimerization is necessary for the binding of HIV-1 Env to hDC-SIGN.^{15,35} In contrast, the DC-SIGNS expressed on the mammalian cells underwent protein modification and folding in the endoplasmic reticulum (ER), as well as further membrane trafficking, in order to be sorted to cell surface. Thus, it is conceivable that the structure of membrane displayed DC-SIGN presented on the 293T surface might be different from that of soluble DC-SIGN, thereby masking binding epitopes present *in vitro* and preventing several of our selected e10Fn3 variants from binding. In this regard, it remains interesting to investigate whether it is viable and perhaps more efficient for a selection directly against DC-SIGN expressed on the mammalian cell surface.

Many antitumor and antiviral vaccines require the induction of cytotoxic CD8⁺ T cells.^{37–39} In order to establish CD8⁺ T cell immunity, antigen peptides need to be presented first by the MHC I molecules on APCs and usually require antigens from an endogenous source.³⁶ Exogenous antigens are usually internalized, processed, and presented to CD4⁺ T cells by MHC II molecules.³⁶ However, the generation of CD8⁺ T cell immunity by presentation of exogenous antigen by MHC I can be accomplished by another naturally occurring pathway: when

exogenous antigens are internalized into cells and later processed by proteasomes through a process termed cross-presentation.⁴⁰ Therefore, it was important to evaluate whether eFn-DC6-mediated antigen delivery could trigger the cross-presentation function of APCs and, hence, stimulate antigen-specific CD8⁺ T responses. For this purpose, we chose a MHC I-restricted epitope derived from the influenza matrix protein that is specific for human HLA-A2⁺ as a model antigen for the study.³³ Because most humans have been previously exposed to influenza virus, most human sources of HLA-A2⁺ PBMCs contain CD8⁺ T cells reactive to the chosen epitope peptide. This antigen peptide was fused to the C terminus of eFn-DC6 or eFn-WT to generate chimeric molecules for DC-SIGN-targeted antigen delivery (Figure 6A). From the co-culture experiment, the eFn-DC6-Ag group showed much higher responses than those of the eFn-WT-Ag group (Figure 6B). These data confirmed that antigen delivered via eFn-DC6-mediated targeting of DC-SIGN could be cross-presented by DCs, resulting in CD8⁺ T cell responses. Although the mechanism of eFn-DC6-mediated cross-presentation remains elusive,³⁶ we speculate that binding of eFn-DC6 to DC-SIGN induces internalization of antigens to endosomes. Through egress from the endosomal compartment, antigens leak into the cytosol, where they gain access to the ER-based class I process machinery.^{40,41} A similar mechanism could be used to explain the CD8⁺ T cell responses generated by antibody-mediated antigen delivery to the type I C-type lectin mannose receptor (MR)⁴² and DEC-205.⁴³

In conclusion, we constructed a library by randomizing two loops of an enhanced fibronectin scaffold (e10Fn3) and exploited the mRNA display method to successfully identify an e10Fn3 variant, eFn-DC6, which possesses high specificity and affinity to hDC-SIGN and moderate affinity to mDC-SIGN. This ligand was found to enter cells in a more clathrin-dependent pathway. As an antigen carrier, we demonstrated that eFn-DC6 was able to direct antigen delivery to DCs and mediate cross-presentation of antigens to elicit class I-based cytotoxic CD8⁺ T cell responses *in vitro*. Taken together, this study demonstrates the feasibility of using mRNA display selection as a method of identifying high-affinity ligands as vaccine carriers for targeted delivery of antigens to DCs, thus paving the way for the design of novel molecules able to target other C-type lectins for DC-directed immunization.

METHODS

Cloning, Expression, and Purification of hDC-SIGN and mDC-SIGN. The cDNAs for the extracellular domain (ECD) of hDC-SIGN and mDC-SIGN were PCR-amplified from plasmids FUW-mDCSIGN and FUW-hDCSIGN.¹⁶ The PCR reaction also introduced a BirA biotinylation recognition sequence at the 5'-end. The cDNAs were then separately cloned into the pET302/NT-His vector (Life Technologies, Grand Island, NY). In order to add biotin to the target protein, BL21(DE3) was first transformed with plasmid pBirAcm, which was purified from *E. coli* strain EVB101 (Avidity, Aurora, CO) and able to express biotin ligase under isopropyl- β -D-thiogalactoside (IPTG) induction, followed by further transformation with pET302/NT-His plasmid vectors containing either hDC-SIGN or mDC-SIGN ECD. Bacteria were inoculated in 1 L of Luria Broth supplemented with 100 μ g mL⁻¹ of ampicillin and 10 μ g mL⁻¹ of chloramphenicol and grown at 37 $^{\circ}$ C with shaking. When the growth of bacteria reached the midlog phase at 37 $^{\circ}$ C, protein expression was induced with IPTG at a final concentration of 1 mM, and free biotin (Sigma-Aldrich, St. Louis, MO) was added to a final concentration of 50 μ M. The induced cultures were incubated for another 4 h before the cells were harvested by centrifuging at 6,000 \times g for 10 min at 4

°C. The resulting cell pellet was resuspended in 15 mL of 100 mM NaH_2PO_4 , pH 8.0, 10 mM Tris-HCl, and 6 M guanidine HCl and then lysed by French press. The lysate was supplemented with 0.01% β -mercaptoethanol, incubated at 4 °C for 2 h and then centrifuged at $150,000 \times g$ for 30 min at 4 °C in a Beckman JA-25 rotor. The supernatant was incubated with 1 mL of nickel-nitrilotriacetic acid-agarose (Qiagen, Valencia, CA) (pre-equilibrated with denaturing buffer) at 4 °C overnight. The resins were loaded onto a chromatography column, and all subsequent washes were done with a 20-fold resin-volume excess of wash buffer (30 mM Tris-HCl, pH 8.0, 0.5 M NaCl, 1 mM CaCl_2 , 6 M urea, and 10 mM imidazole). Successive washes using the buffer (30 mM Tris-HCl, pH 8.0, 0.5 M NaCl) with decreasing concentrations of urea starting from 6 M urea were performed to refold the proteins. The renatured proteins were eluted with the elution buffer (30 mM Tris-HCl, pH 8.0, 0.5 M NaCl, 1 mM CaCl_2 , and 1 M imidazole) and exchanged into PBS buffer using a PD-10 column (GE Healthcare, Pittsburgh, PA).

An Fc-gp120-based ELISA was used to confirm the binding function of refolded hDC-SIGN. ELISA plates were coated with 10 μg purified hDC-SIGN or mDC-SIGN ECD in each well. After blocking, the plates were then incubated with different concentrations of Fc-gp120 protein ranging from 0 to 300 nM. After washing, the plates were incubated with HRP-conjugated anti-human IgG antibody, and the reaction was visualized by chromogenic substrate (TMB) and stopped by 1 M H_2SO_4 . Absorbance at 450 nm was measured with reduction at 650 nm using an ELISA plate reader.

e10Fn3 Library Construction. Construction of an antibody-mimetic e10Fn3 library using eight oligonucleotides synthesized by the Yale Keck Oligonucleotide Synthesis facility or Integrated DNA Technologies has been described previously.⁴⁴ Briefly, the e10Fn3 library differs from the human 10th fibronectin type III domain because the e10Fn3 library is truncated at the N-terminus and contains 5 scaffold mutations that increase expression and/or solubility (VSK, A6E, T8S, L12I, and L13Q), and the last position of the BC loop is restricted to Leu, Ile, or Val for higher structural stability.²⁸

Three oligonucleotides, eFnoligo1, 2, and 3, were newly designed for introducing the mutations and the doped last position of BC loop into e10Fn3 library. Briefly, eFnoligo3 (5'-ACC AGC ATC CAG ATC AGC TGG 5SS 5SS 5SS 5SS 5SS 5SS VTT CGC TAC TAC CGC ATC ACC TAC G-3'; 5 indicated the dNTP mixture of 20% T, 30% C, 30% A, and 20% G; S were mixed with 60% C and 40% G; V denoted the mixture of C, A, and G equally), containing the randomized BC loop was used to introduce two mutations (L12I and L13Q) and one doped residue. eFnoligo3 was annealed to Fnoligo4, extended by Klenow DNA polymerase, and purified by agarose gel electrophoresis. The purified product was PCR amplified using the second new primer, eFnoligo2 (5'-CAA TTA CAA TGC TCG AGG TCA AGG AAG CAT CAC CAA CCA GCA TCC AGA TCA GCT GG-3') and Fnoligo5. eFnoligo2 was used to insert three mutations, VSK, A6E, and T8S, into the N-terminus of e10FnIII library. Fnoligo6 and Fnoligo7 containing the randomized FG loop were annealed and extended by Klenow DNA polymerase. All PCR and Klenow products were purified by agarose gel electrophoresis.

Both BC and FG fragments were digested with Bsa I and purified by agarose gel electrophoresis. Purified BC and FG fragments were ligated together using T4 DNA ligase and purified by agarose gel electrophoresis where 13 ng/ μL of ligated product was recovered. The approximate theoretical complexity of e10FnIII library is 10^{12} (1 trillion unique sequences). The library was extended and amplified by the third new oligonucleotide, eFnoligo1 (5'-TTC TAA TAC GAC TCA CTA TAG GGA CAA TTA CTA TTT ACA ATT ACA ATG CTC GAG GTC AAG G-3'), and Fnoligo9 (5'-GGA GCC GCT ACC CTT ATC GTC GTC ATC CTT GTA ATC GGA TCC GGT GCG GTA GTT GAT GGA GAT CG-3') in a 10-mL PCR reaction.

mRNA Display. The first round of selection was started by PCR amplification (1.5 mL) of the naïve e10Fn3 library to obtain a library with ~ 10 copies of the theoretical 10^{12} independent sequences. The PCR product was used as the template in a 1.5 mL *in vitro* transcription reaction using T7 RNA polymerase at 37 °C for 2 h to generate mRNA. The transcription reaction was terminated with the

addition of 1/10th of the reaction volume of 0.5 M EDTA at pH 8.0. The RNA was purified by Urea PAGE electrophoresis, electroelution, and ethanol precipitation. Purified RNA was ligated with the DNA linker-puromycin, pF30P (5'-phosphate-dA₂₁₋₉-3-dAdCdC-Pu, where 9 is phosphoramidite spacer 9, Pu is puromycin CPG, and the 5'-end was phosphorylated using chemical phosphorylation reagent I; Glen Research Corp.), with a splint oligo, FN-pF30P-Splint (5'-TTT TTT TTT TTT GGA GCC GCT ACC-3', which is complementary to the 3' end of the RNA library and the 5' end of pF30P) and T4 DNA ligase in a 1.0 mL reaction at RT for 1 h. The library of mRNA-protein fusions was created via a 2.5 mL *in vitro* translation reaction in rabbit reticulocyte lysate (Green Hectares; salts and buffers from Novagen) where purified RNA-pF30P was translated at 30 °C for 1 h. To enhance fusion formation, 10 μL of salt mixture (2 μL of 1 M MgCl_2 and 8 μL of 2.5 M KCl) was added to each 25 μL of translation and incubated at RT for 15 min. Fusions were purified with Oligo(dT) Cellulose Type 7 (GE Healthcare Life Science) in dT buffer (100 mM Tris-HCl, pH 8.0, 1 M NaCl, 0.2% Triton X-100, and 1 mM EDTA) at 4 °C for 1 h and then eluted with RT ddH₂O. The elution, containing purified fusions, was desalted and exchanged with the first strand buffer (50 mM Tris-HCl, pH 8.3, 75 mM KCl, and 3 mM MgCl_2), using a 5 mL NAP-25 column (GE Healthcare Life Science). The purified fusions were then reverse transcribed with reverse primer Fnoligo10 (5'-GGA GCC GCT ACC CTT ATC GTCG-3'), using Superscript II enzyme (Invitrogen, Carlsbad, CA) at 42 °C for 1 h to generate cDNA/mRNA-protein fusions for selection.

N-Terminal biotin-tagged mDC-SIGN proteins were immobilized on acrylamide-streptavidin beads (Pierce, Thermo Scientific, Rockford, IL) at RT for 1 h immediately prior to the selection. mDC-SIGN-immobilized beads were resuspended in selection buffer (50 mM Tris-HCl, pH 8.0, 150 mM NaCl, 0.02% (v/v) Tween-20, 0.5 mg mL⁻¹ BSA, and 0.1 mg mL⁻¹ tRNA) and incubated with the cDNA/mRNA-protein fusion library at 4 °C for 1 h. After incubation, the beads were washed 4 times with selection buffer and subjected to PCR to amplify bound fusions. The PCR product was labeled as pool 1 and used to make the fusions for the next round of selection. From the second round of selection, the volume of translation reaction was reduced to 100 μL , and FLAG purification was applied to purify full-length fusions. After reverse transcription, C-terminal FLAG-tagged fusions were pulled down with anti-FLAG M2 agarose beads (Sigma) at 4 °C for 1 h and eluted with the FLAG peptide (Sigma) twice at RT. A preclear step was also introduced to exclude nonspecific bead binders immediately before selection. The FLAG-purified fusions were flowed through 100 μL of D-biotin treated resin packed in small column. After two rounds of selection, the beads were switched to agarose-neutravidin beads (Pierce) to avoid bead background binding. The selection was the same for hDC-SIGN, except that hDC-SIGN ECD was used as the target. A four-round selection was performed against hDC-SIGN for a total of seven rounds of selection.

In Vitro Radiolabeled Binding Assay. The affinity of each pool was monitored by pull-down of radiolabeled fusions against mDC-SIGN or hDC-SIGN immobilized on beads. L-[³⁵S]Methionine (MP Biomedicals) was used to replace cold methionine in the translation reaction. After translation, the reaction was treated with ribonuclease A (Roche Applied Science) to generate pF30P-linked e10Fn3s. The radiolabeled fusions were incubated with mDC-SIGN-immobilized beads, hDC-SIGN-immobilized beads, or beads without target at 4 °C for 1 h. The beads were washed 4 times with selection buffer and resuspended with ddH₂O. The radioactivity present in the flow through, four washes, and beads was detected by scintillation counting. The total input of radiolabeled fusion added to the binding reaction was the total of flow through, wash, and bead counts. The percent binding of each pool was calculated by the ratio of bead counts/total input counts.

The final M3H4 pool was PCR amplified and introduced with two restriction sites, Xho I and BamHI, using eFnoligo1 and Fnoligo11 as primers. The PCR products were cloned into vector pAO5 by restriction digestion and ligation. Twenty colonies were cultured, sequenced, and grouped by the similarity of sequences, resulting in seven clones where two clones has high copy numbers and five

singletons. They were further tested for the affinity using the *in vitro* radiolabeled binding assay. The selected clones were first PCR amplified using eFnloligo1 and Fnloligo9 and then subjected to *in vitro* transcription to make mRNA. mRNA from each clone was translated in rabbit reticulocyte lysate supplemented with L-[³⁵S]methionine to generate radiolabeled proteins. The radiolabeled proteins were purified by pull down with anti-FLAG M2 beads and elution with 3X FLAG peptides. The binding of purified radiolabeled proteins and the data analysis were the same as pool binding assay.

Cloning, Expression, and Purification of Wild-Type e10Fn3 (eFn-WT) and Selected eFn-DC Clones with C-terminal HA Tag or Influenza Antigen Peptide. For the cell binding assay, a HA tag (YPYDVPDYA) was cloned onto the C-terminus of eFn-WT and selected clones from the pools (eFn-DC1, eFn-DC2, eFn-DC3, eFn-DC4, and eFn-DC6) in the pAO5 vector. Bacterial protein expression and purification were optimized and conducted according to the Qiagen protocol for purification under native conditions. Influenza antigen peptide sequence was introduced following e10Fn3 and flanked by arginines and a His tag ((e10Fn3)-RR-GILGFVFTL-RRR-HHHHH). The influenza peptide is derived from the influenza A matrix protein, representing the HLA-A*0201 (human MHC class I molecule)-restricted epitope.³³ The arginines were added to increase the proteasomal digestion during processing of peptides that will be presented via the MHC class I.^{29,34} All of these constructs were expressed and purified using the same protocols as the HA-tagged protein.

Cell Functional Assay: Binding, Internalization. 293T.hDCSIGN and 293T.mDCSIGN cells were described previously.¹⁶ Five HA-tagged eFn-DC proteins (eFn-DC1, eFn-DC2, eFn-DC3, eFn-DC4, and eFn-DC6) and HA-tagged eFn-WT were tested. For the binding test, cells were treated with 10 nM of HA-tagged e10Fn3s at 4 °C for 30 min. The treated cells were then washed with PBS and incubated with rabbit anti-HA antibody (Abcam, Cambridge, MA) at 4 °C for 10 min. After incubation, the resulting cells were immunostained with allophycocyanin (APC)-conjugated anti-rabbit IgG (Invitrogen) and analyzed via flow cytometry (BD; data were analyzed using Flowjo). The approximate K_D of eFn-DC6 was determined by treating 293T.hDCSIGN or 293T.mDCSIGN cells with 0.4–800 nM of eFn-DC6, followed by analysis using flow cytometry, as described previously.⁴⁵ The internalization induced by eFn-DC6 was tested by first incubating the 293T.hDCSIGN cells with 100 nM of HA-tagged eFn-DC6 at 4 °C for 30 min in duplicate. After the unbound e10Fn3s were washed off, one sample was cultured at 37 °C for another 2 h to induce internalization, while the duplicate was kept at 4 °C as a noninternalizing control. Then, cell-surface staining for HA tag was performed, and the difference of fluorescence intensity between 4 and 37 °C was calculated to obtain the internalization efficiency.^{15,29} PE-conjugated anti-human DC-SIGN antibody was obtained from BioLegend (clone 9E9A8).

Confocal Imaging. Fluorescence images were acquired on a Yokogawa spinning-disk confocal scanner system (Solamere Technology Group, Salt Lake City, UT) using a Nikon eclipse Ti-E microscope equipped with a 60×/1.49 Apo TIRF oil objective and a Cascade II: 512 EMCCD camera (Photometrics, Tucson, AZ, USA). An AOTF (acousto-optical tunable filter)-controlled laser-merge system (Solamere Technology Group Inc.) was used to provide illumination power at each of the following laser lines: 491, 561, and 640 nm solid-state lasers (50mW for each laser). Image processing and data analysis were carried out using the Nikon NIS-Elements software. To quantify the extent of colocalization, Mander's overlap coefficients were generated using the Nikon NIS-Elements software by viewing more than 50 cells at each time point. For the colocalization study, endocytic markers, 293T.hDC-SIGN cells or iDCs were seeded on glass bottom dishes (MatTek Corporation, Ashland, MA) and grown at 37 °C overnight. The cells were then incubated with 100 nM HA-tagged eFn-DC6 for 30 min at 4 °C to synchronize internalization. After being washed with PBS, the treated cells were then warmed to 37 °C to initiate particle internalization for the indicated time periods. The cells were fixed, permeabilized with 0.1% Triton X-100, and then immunostained with the corresponding antibodies specific to clathrin,

caveolin-1, or EEA1 (Santa Cruz Biotech., Santa Cruz, CA), followed by counterstaining with DAPI (Invitrogen). Secondary antibody Alexa488-conjugated goat anti-mouse immunoglobulin G (IgG) and Alexa594-conjugated anti-rabbit IgG antibodies were purchased from Invitrogen (Carlsbad, CA). Mander's overlap coefficient was calculated using more than 40 areas for each experiment.

Generation of Human DCs from Human PBMCs and Mouse DCs from Mouse Bone Marrow. Human PBMC-derived DCs were generated and purified as previously described,^{46,47} except that human PBMCs were from HLA-A2⁺ patients (AllCells, LLC.). Briefly, plastic-adherent cell fractions of human PBMCs were grown in RPMI 1640 with 10% heat-inactivated FBS, 2 mM L-glutamine, 100 U mL⁻¹ penicillin, 100 μg mL⁻¹ streptomycin, 1000 IU mL⁻¹ GM-CSF, and 1000 IU mL⁻¹ IL-4 (PeproTech, Rocky Hill, NJ) for 6 days with media carefully changed every 2 days. For mouse BMDC, we employed a previously described procedure to generate bone marrow-derived DCs (BMDCs) with various genetic backgrounds. Briefly, bone marrow from the femurs and tibias of mice was grown in RPMI 1640 with 10% heat-inactivated FBS, 2 mM L-glutamine, 100 U mL⁻¹ penicillin, 100 μg mL⁻¹ streptomycin, 0.05 mM 2-ME, and 20 ng mL⁻¹ GM-CSF (J558L supernatant) after the red blood cells were lysed. Cultures were initiated by placing 10⁷ bone marrow cells in 10 mL of medium onto 100-mm Petri dishes (Falcon 1029 plates; BD Labware, Franklin Lakes, NJ). On day 3, another 10 mL of J558L-conditioned medium was added. On day 6, suspension cells were collected.

Enzyme-Linked-Immunospot (ELISPOT) Assay of DCs Co-cultured with Autologous PBMCs. On day 6 of DC development, eFn-DC6 fused influenza peptide (eFn-DC6-Ag), eFn-WT fused influenza peptide (eFn-WT-Ag), eFn-DC6 or GILGFVFTL peptide antigen was added to the culture for 24 h. The ELISPOT assay was performed according to a previous report⁴⁸ with some modifications. Briefly, anti-human IFN-γ antibody (10 μg mL⁻¹ in PBS, clone MD-1, BioLegend) was used as the capture antibody and plated with 100 μL/well on 96-well MultiScreen-IP plates (Millipore) overnight at 4 °C. The plate was decanted and blocked with the RPMI medium containing 10% FBS at 37 °C for 2 h. On day 7, DCs treated with different e10Fn3s were washed separately and cultured with freshly thawed autologous PBMCs (2 × 10⁶ PBMCs co-cultured with 4 × 10⁵ DCs in each well). After 60 h of incubation at 37 °C, cells were lysed, and plates were detected by 1 μg mL⁻¹ biotinylated anti-IFN-γ antibody (clone 4S.B3, BioLegend) for 2 h at RT. Plates were further washed and incubated with the 1,000-fold-diluted streptavidin-alkaline phosphatase conjugate for 45 min at RT. After a final extensive wash, spots were identified by adding BCIP/NBTplus substrate (Millipore), and the number of IFN-γ-producing cells was quantified by an ELISPOT reader.

AUTHOR INFORMATION

Corresponding Author

*E-mail: richard.roberts@usc.edu; pinwang@usc.edu.

Author Contributions

#These authors contributed equally to this work.

Notes

The authors declare no competing financial interest.

ACKNOWLEDGMENTS

We would like to thank C. Anders for his help in e10Fn3 library construction and J. Zhao for the gift of the wild-type e10Fn3 clone. This work was supported by grants from the National Institutes of Health (R01AI68978 and P01CA132681) and a translational acceleration grant from the Joint Center for Translational Medicine.

ABBREVIATIONS

DC, dendritic cell; APC, antigen-presenting cell; DC-SIGN, DC-specific intercellular adhesion molecule grabbing non-integrin; PBMC, peripheral blood mononuclear cell; ECD,

extracellular domain; CLR, C-type lectin receptor; CRD, carbohydrate recognition domain; EEA-1, Early Endosome Antigen-1

REFERENCES

- (1) Mellman, I., and Steinman, R. M. (2001) Dendritic cells: specialized and regulated antigen processing machines. *Cell* 106, 255–258.
- (2) Fajardo-Moser, M., Berzel, S., and Moll, H. (2008) Mechanisms of dendritic cell-based vaccination against infection. *Int. J. Med. Microbiol.* 298, 11–20.
- (3) Wei, H., Wang, H., Lu, B., Li, B., Hou, S., Qian, W., Fan, K., Dai, J., Zhao, J., and Guo, Y. (2008) Cancer immunotherapy using in vitro genetically modified targeted dendritic cells. *Cancer Res.* 68, 3854–3862.
- (4) Boudreau, J. E., Bonehill, A., Thielemans, K., and Wan, Y. (2011) Engineering dendritic cells to enhance cancer immunotherapy. *Mol. Ther.* 19, 841–853.
- (5) Cheever, M. A., and Higano, C. S. (2011) PROVENGE (Sipuleucel-T) in prostate cancer: the first FDA-approved therapeutic cancer vaccine. *Clin. Cancer Res.* 17, 3520–3526.
- (6) Kantoff, P. W., Higano, C. S., Shore, N. D., Berger, E. R., Small, E. J., Penson, D. F., Redfern, C. H., Ferrari, A. C., Dreicer, R., Sims, R. B., Xu, Y., Frohlich, M. W., and Schellhammer, P. F. (2010) Sipuleucel-T immunotherapy for castration-resistant prostate cancer. *N. Engl. J. Med.* 363, 411–422.
- (7) Plosker, G. L. (2011) Sipuleucel-T: in metastatic castration-resistant prostate cancer. *Drugs* 71, 101–108.
- (8) Hammerstrom, A. E., Cauley, D. H., Atkinson, B. J., and Sharma, P. (2011) Cancer immunotherapy: sipuleucel-T and beyond. *Pharmacotherapy* 31, 813–828.
- (9) Tacken, P. J., de Vries, I. J., Torensma, R., and Figdor, C. G. (2007) Dendritic-cell immunotherapy: from ex vivo loading to in vivo targeting. *Nat. Rev. Immunol.* 7, 790–802.
- (10) Figdor, C. G., van Kooyk, Y., and Adema, G. J. (2002) C-type lectin receptors on dendritic cells and Langerhans cells. *Nat. Rev. Immunol.* 2, 77–84.
- (11) Geijtenbeek, T. B., Torensma, R., van Vliet, S. J., van Duijnhoven, G. C., Adema, G. J., van Kooyk, Y., and Figdor, C. G. (2000) Identification of DC-SIGN, a novel dendritic cell-specific ICAM-3 receptor that supports primary immune responses. *Cell* 100, 575–585.
- (12) Tacken, P. J., de Vries, I. J., Gijzen, K., Joosten, B., Wu, D., Rother, R. P., Faas, S. J., Punt, C. J., Torensma, R., Adema, G. J., and Figdor, C. G. (2005) Effective induction of naive and recall T-cell responses by targeting antigen to human dendritic cells via a humanized anti-DC-SIGN antibody. *Blood* 106, 1278–1285.
- (13) Park, C. G., Takahara, K., Umemoto, E., Yashima, Y., Matsubara, K., Matsuda, Y., Clausen, B. E., Inaba, K., and Steinman, R. M. (2001) Five mouse homologues of the human dendritic cell C-type lectin, DC-SIGN. *Int. Immunol.* 13, 1283–1290.
- (14) Powlesland, A. S., Ward, E. M., Sadhu, S. K., Guo, Y., Taylor, M. E., and Drickamer, K. (2006) Widely divergent biochemical properties of the complete set of mouse DC-SIGN-related proteins. *J. Biol. Chem.* 281, 20440–20449.
- (15) Takahara, K., Yashima, Y., Omatsu, Y., Yoshida, H., Kimura, Y., Kang, Y. S., Steinman, R. M., Park, C. G., and Inaba, K. (2004) Functional comparison of the mouse DC-SIGN, SIGNR1, SIGNR3 and Langerin, C-type lectins. *Int. Immunol.* 16, 819–829.
- (16) Yang, L., Yang, H., Rideout, K., Cho, T., Joo, K. I., Ziegler, L., Elliot, A., Walls, A., Yu, D., Baltimore, D., and Wang, P. (2008) Engineered lentivector targeting of dendritic cells for in vivo immunization. *Nat. Biotechnol.* 26, 326–334.
- (17) Dai, B., Yang, L., Yang, H., Hu, B., Baltimore, D., and Wang, P. (2009) HIV-1 Gag-specific immunity induced by a lentivector-based vaccine directed to dendritic cells. *Proc. Natl. Acad. Sci. U.S.A.* 106, 20382–20387.
- (18) Xiao, L., Kim, J., Lim, M., Dai, B., Yang, L., Reed, S. G., Baltimore, D., and Wang, P. (2012) A TLR4 agonist synergizes with dendritic cell-directed lentiviral vectors for inducing antigen-specific immune responses. *Vaccine* 30, 2570–2581.
- (19) Yang, H., Hu, B., Xiao, L., and Wang, P. (2011) Dendritic cell-directed lentivector vaccine induces antigen-specific immune responses against murine melanoma. *Cancer Gene Ther.* 18, 370–380.
- (20) Roberts, R. W., and Szostak, J. W. (1997) RNA-peptide fusions for the in vitro selection of peptides and proteins. *Proc. Natl. Acad. Sci. U.S.A.* 94, 12297–12302.
- (21) Takahashi, T. T., and Roberts, R. W. (2009) In vitro selection of protein and peptide libraries using mRNA display. *Methods Mol. Biol.* 535, 293–314.
- (22) Takahashi, T. T., Austin, R. J., and Roberts, R. W. (2003) mRNA display: ligand discovery, interaction analysis and beyond. *Trends Biochem. Sci.* 28, 159–165.
- (23) Hayashi, Y., Morimoto, J., and Suga, H. (2012) In vitro selection of anti-Akt2 thioether-macrocytic peptides leading to isoform-selective inhibitors. *ACS Chem. Biol.* 7, 607–613.
- (24) Jackrel, M. E., Cortajarena, A. L., Liu, T. Y., and Regan, L. (2010) Screening libraries to identify proteins with desired binding activities using a split-GFP reassembly assay. *ACS Chem. Biol.* 5, 553–562.
- (25) Olson, C. A., Liao, H. I., Sun, R., and Roberts, R. W. (2008) mRNA display selection of a high-affinity, modification-specific phospho-IkappaBalpha-binding fibronectin. *ACS Chem. Biol.* 3, 480–485.
- (26) Xu, L., Aha, P., Gu, K., Kuimelis, R. G., Kurz, M., Lam, T., Lim, A. C., Liu, H., Lohse, P. A., Sun, L., Weng, S., Wagner, R. W., and Lipovsek, D. (2002) Directed evolution of high-affinity antibody mimics using mRNA display. *Chem. Biol.* 9, 933–942.
- (27) Koide, A., Bailey, C. W., Huang, X. L., and Koide, S. (1998) The fibronectin type III domain as a scaffold for novel binding proteins. *J. Mol. Biol.* 284, 1141–1151.
- (28) Olson, C. A., Adams, J. D., Takahashi, T. T., Qi, H., Howell, S. M., Wu, T. T., Roberts, R. W., Sun, R., and Soh, H. T. (2011) Rapid mRNA-display selection of an IL-6 inhibitor using continuous-flow magnetic separation. *Angew. Chem., Int. Ed.* 50, 8295–8298.
- (29) Dakappagari, N., Maruyama, T., Renshaw, M., Tacken, P., Figdor, C., Torensma, R., Wild, M. A., Wu, D., Bowdish, K., and Kretz-Rommel, A. (2006) Internalizing antibodies to the C-type lectins, L-SIGN and DC-SIGN, inhibit viral glycoprotein binding and deliver antigen to human dendritic cells for the induction of T cell responses. *J. Immunol.* 176, 426–440.
- (30) Cambi, A., Beeren, I., Joosten, B., Fransen, J. A., and Figdor, C. G. (2009) The C-type lectin DC-SIGN internalizes soluble antigens and HIV-1 virions via a clathrin-dependent mechanism. *Eur. J. Immunol.* 39, 1923–1928.
- (31) Joo, K. I., Lei, Y. N., Lee, C. L., Lo, J., Xie, J. S., Hamm-Alvarez, S. F., and Wang, P. (2008) Site-specific labeling of enveloped viruses with quantum dots for single virus tracking. *ACS Nano* 2, 1553–1562.
- (32) Tacken, P. J., Ginter, W., Berod, L., Cruz, L. J., Joosten, B., Sparwasser, T., Figdor, C. G., and Cambi, A. (2011) Targeting DC-SIGN via its neck region leads to prolonged antigen residence in early endosomes, delayed lysosomal degradation, and cross-presentation. *Blood* 118, 4111–4119.
- (33) Nijman, H. W., Houbiers, J. G., Vierboom, M. P., van der Burg, S. H., Drijfhout, J. W., D'Amaro, J., Kenemans, P., Melief, C. J., and Kast, W. M. (1993) Identification of peptide sequences that potentially trigger HLA-A2.1-restricted cytotoxic T lymphocytes. *Eur. J. Immunol.* 23, 1215–1219.
- (34) Sundaram, R., Sun, Y., Walker, C. M., Lemonnier, F. A., Jacobson, S., and Kaumaya, P. T. (2003) A novel multivalent human CTL peptide construct elicits robust cellular immune responses in HLA-A*0201 transgenic mice: implications for HTLV-1 vaccine design. *Vaccine* 21, 2767–2781.
- (35) Bernhard, O. K., Lai, J., Wilkinson, J., Sheil, M. M., and Cunningham, A. L. (2004) Proteomic analysis of DC-SIGN on

dendritic cells detects tetramers required for ligand binding but no association with CD4. *J. Biol. Chem.* 279, 51828–51835.

(36) Trombetta, E. S., and Mellman, I. (2005) Cell biology of antigen processing in vitro and in vivo. *Annu. Rev. Immunol.* 23, 975–1028.

(37) Kagi, D., Vignaux, F., Ledermann, B., Burki, K., Depraetere, V., Nagata, S., Hengartner, H., and Golstein, P. (1994) Fas and perforin pathways as major mechanisms of T cell-mediated cytotoxicity. *Science* 265, 528–530.

(38) Tanaka, H., Yoshizawa, H., Yamaguchi, Y., Ito, K., Kagamu, H., Suzuki, E., Gejyo, F., Hamada, H., and Arakawa, M. (1999) Successful adoptive immunotherapy of murine poorly immunogenic tumor with specific effector cells generated from gene-modified tumor-primed lymph node cells. *J. Immunol.* 162, 3574–3582.

(39) Wong, P., and Pamer, E. G. (2003) CD8 T cell responses to infectious pathogens. *Annu. Rev. Immunol.* 21, 29–70.

(40) Ackerman, A. L., and Cresswell, P. (2004) Cellular mechanisms governing cross-presentation of exogenous antigens. *Nat. Immunol.* 5, 678–684.

(41) Guermonprez, P., Saveanu, L., Kleijmeer, M., Davoust, J., Van Endert, P., and Amigorena, S. (2003) ER-phagosome fusion defines an MHC class I cross-presentation compartment in dendritic cells. *Nature* 425, 397–402.

(42) Ramakrishna, V., Trembl, J. F., Vitale, L., Connolly, J. E., O'Neill, T., Smith, P. A., Jones, C. L., He, L. Z., Goldstein, J., Wallace, P. K., Keler, T., and Endres, M. J. (2004) Mannose receptor targeting of tumor antigen pmel17 to human dendritic cells directs anti-melanoma T cell responses via multiple HLA molecules. *J. Immunol.* 172, 2845–2852.

(43) Bonifaz, L., Bonnyay, D., Mahnke, K., Rivera, M., Nussenzweig, M. C., and Steinman, R. M. (2002) Efficient targeting of protein antigen to the dendritic cell receptor DEC-205 in the steady state leads to antigen presentation on major histocompatibility complex class I products and peripheral CD8+ T cell tolerance. *J. Exp. Med.* 196, 1627–1638.

(44) Olson, C. A., and Roberts, R. W. (2007) Design, expression, and stability of a diverse protein library based on the human fibronectin type III domain. *Protein Sci.* 16, 476–484.

(45) Benedict, C. A., MacKrell, A. J., and Anderson, W. F. (1997) Determination of the binding affinity of an anti-CD34 single-chain antibody using a novel, flow cytometry based assay. *J. Immunol. Methods* 201, 223–231.

(46) Sallusto, F., and Lanzavecchia, A. (1994) Efficient presentation of soluble antigen by cultured human dendritic cells is maintained by granulocyte/macrophage colony-stimulating factor plus interleukin 4 and downregulated by tumor necrosis factor alpha. *J. Exp. Med.* 179, 1109–1118.

(47) Romani, N., Gruner, S., Brang, D., Kampgen, E., Lenz, A., Trockenbacher, B., Konwalinka, G., Fritsch, P. O., Steinman, R. M., and Schuler, G. (1994) Proliferating dendritic cell progenitors in human blood. *J. Exp. Med.* 180, 83–93.

(48) Hoffmann, T. K., Meidenbauer, N., Dworacki, G., Kanaya, H., and Whiteside, T. L. (2000) Generation of tumor-specific T-lymphocytes by cross-priming with human dendritic cells ingesting apoptotic tumor cells. *Cancer Res.* 60, 3542–3549.